

Anharmonic lattice vibrations in palladium

This article has been downloaded from IOPscience. Please scroll down to see the full text article.

1990 J. Phys.: Condens. Matter 2 8859

(<http://iopscience.iop.org/0953-8984/2/45/002>)

View [the table of contents for this issue](#), or go to the [journal homepage](#) for more

Download details:

IP Address: 171.66.16.151

The article was downloaded on 11/05/2010 at 06:58

Please note that [terms and conditions apply](#).

Anharmonic lattice vibrations in palladium

Marco Zoli†

Institut für Theoretische Physik, Universität Hamburg, Jungiusstrasse 9,
2000 Hamburg 36, Federal Republic of Germany

Received 26 February 1990, in final form 25 June 1990

Abstract. Macroscopic and microscopic effects of anharmonic lattice vibrations in Pd have been studied. The interatomic forces are modelled according to a phenomenological potential which includes three-body angular forces in the harmonic part. The cubic and quartic force constants are fitted to the experimental linear thermal expansion coefficient and constant-pressure specific heat, respectively. Thermoelastic properties are evaluated in quasi-harmonic approximation while caloric properties require computation of constant-volume anharmonic contributions. The phonon lineshifts and linewidths have been calculated along the principal symmetry directions, in the framework of the second-order perturbation theory. The room-temperature experimental anomalies in the $[\xi\xi 0]T_1$ branch are reproduced by the theory.

1. Introduction

In this paper, I address both macroscopic and microscopic effects of the anharmonic interactions in Pd. For this metal, detailed experimental investigations of lattice dynamics have been carried out at several temperatures by the use of inelastic neutron scattering techniques. Miiller and Brockhouse (1968, 1971) first pointed out the existence of anomalous shifts in the phonon frequencies along the $[\xi\xi 0]T_1$ branch at reduced wavevectors $\xi \simeq 0.3$ – 0.4 . These anomalies have been correlated (Miiller 1975) with possible Kohn transitions (Kohn 1959) across the ‘heavy’ hole Fermi sheet formed from the fifth band electrons. Associated with virtual scattering of conduction electrons by the lattice vibrations, are real Kohn transitions which contribute to an increase in phonon linewidths. Such broadenings have been in fact observed for transverse modes by Miiller (1975) and in low-temperature longitudinal modes by Youngblood *et al* (1979). Pinski and Butler (1979) have attributed these experimental features to an enhanced decay of phonon modes into electron–hole pairs: they have computed the electron–phonon matrix elements within the rigid muffin-tin approximation and have estimated an electron–phonon coupling constant which would lead (in the absence of competing effects such as magnetic fluctuations) to a superconducting transition temperature of 0.3 K. This theoretical model emphasizes the presence of many-body effects which are believed to be strong in Pd.

In recent years, there has been a considerable amount of work devoted to the study of many-body interatomic forces in metals. In the embedded atom method (EAM)

† On leave from Dipartimento di Fisica, Università di Modena, Via Campi 213/A, 41100 Modena, Italy.

(Daw and Baskes 1983), the total energy is modelled as having two contributions: the energy to embed an atom into the local electronic density provided by the remainder of the atoms and an electrostatic term represented by pair interactions. This approach has been widely used to calculate point defects properties (Foiles *et al* 1986), surface relaxations (Ting *et al* 1988) and reconstructions (Ercolessi *et al* 1986), surface and bulk phonons (Daw and Hatcher 1985) of metallic systems. Recently, the EAM has been successfully applied to compute thermal expansion and Gibbs free energy for the solid and liquid phases of FCC metals (Foiles and Adams 1989): the anharmonic effects have been included through the quasi-harmonic approximation (QHA), since the phonon frequencies do depend on the lattice constant.

In a previous paper (Zoli and Bortolani 1990), it was shown that the QHA satisfactorily reproduces the thermoelastic properties of Cu and Al throughout a wide range of temperatures. On the other hand, caloric properties are accurately evaluated only if the constant-volume anharmonic contributions are taken into account. Also the microscopic manifestations of anharmonicity can not be predicted in the framework of the QHA: both phonon linewidths and lineshifts require knowledge of the explicitly temperature dependent anharmonic terms which can be obtained within the constant-volume perturbative theory. In particular, by evaluating the lowest-order diagrams in the phonon self-energy, we have been able to reproduce some anomalous dampings (Zoli *et al* 1990) and lineshifts (Zoli 1990) of phonon modes which are observed in copper and aluminum. Although our theoretical approach attributes to phonon-phonon scattering the major role for such anomalies, we have also taken into account the electron-phonon contribution by using a phenomenological potential with unknown parameters fitted to experimental quantities. In particular, the third- and fourth-order derivatives of the interatomic potential have been related to the experimentally known higher-order elastic constants (HOEC).

In the case of Pd such an approach can not be adopted, since experimental information on the HOEC are, to my knowledge, not available. Alternatively, the experimental thermal expansion and the constant-pressure specific heat can be used to sample the range of the anharmonic potential.

This paper is organized as follows. In section 2, the harmonic model potential is briefly reviewed. In section 3, the thermoelastic and caloric properties are evaluated on the base of the low-order perturbation theory. The volume dependence of the Helmholtz free energy is taken into account. The values of the cubic and quartic force constants are fitted to the experimental linear thermal expansion coefficient and constant-pressure specific heat, respectively. In section 4, the lineshifts and linewidths of transverse and longitudinal phonons are computed along two symmetry directions of the Brillouin zone. The results are discussed in connection with the available experimental data.

2. The harmonic model potential

In calculations of macroscopic and microscopic anharmonic properties, the phonon frequencies and polarisation vectors are assumed to be known. Therefore, it is understood that reliable estimates of anharmonic effects can be carried out once the harmonic part of the potential is built with high accuracy. I have used a force constant harmonic model potential which includes two-body forces up to the sixth-neighbour shell and three-body angular forces restricted to terns of first-neighbour atoms. The harmonic

force constants are determined by a least squares fit to the observed room-temperature phonon frequencies in the high symmetry directions of the Brillouin zone (Miiller and Brockhouse 1971). The range of the two-body harmonic potential is chosen as the one that gives the minimum between the theoretical and the experimental dispersion relations. The experimental second-order elastic constants (SOEC) are also taken into account with an high fitting weight. The relations between SOEC and harmonic force constants are

$$\begin{aligned}
 aC_{11} &= 2(\beta_1 - \alpha_1) + 4(\beta_2 - \alpha_2) + 12(\beta_3 - \alpha_3) + 8(\beta_4 - \alpha_4) + \frac{164}{5}(\beta_5 - \alpha_5) \\
 &\quad + \frac{16}{3}(\beta_6 - \alpha_6) + 12\delta_1 \\
 aC_{12} &= (\beta_1 - \alpha_1) + 6(\beta_3 - \alpha_3) + 4(\beta_4 - \alpha_4) + \frac{18}{5}(\beta_5 - \alpha_5) + \frac{16}{3}(\beta_6 - \alpha_6) - 6\delta_1 \\
 aC_{44} &= aC_{12} + 18\delta_1
 \end{aligned} \tag{1}$$

where a is the lattice constant. The force constants are defined as follows:

$$\alpha_i = \frac{\phi'(r_i)}{r_i} \quad \beta_i = \phi''(r_i) \quad \delta_i = \frac{1}{3a^2} W''(\cos \theta^{JKL}) \tag{2}$$

where i labels the i th-neighbour shell, $\phi(r_i)$ is the pairwise potential and $W(\cos \theta^{JKL})$ is the three-body potential, in which JKL labels the tern of atoms. Since we consider first-neighbour angular forces, it follows that (i) J and L are nearest neighbours of K ; (ii) J and L have to be nearest neighbours of each other.

Table 1. Harmonic and anharmonic force constants values for Pd in units of 10^{12} dyn cm^{-2} ; a is the lattice constant.

$\frac{\beta_1 - \alpha_1}{a}$	$\frac{\delta_1}{a}$	$\frac{\beta_2 - \alpha_2}{a}$	$\frac{\beta_3 - \alpha_3}{a}$	$\frac{\beta_4 - \alpha_4}{a}$	$\frac{\beta_5 - \alpha_5}{a}$	$\frac{\beta_6 - \alpha_6}{a}$
1.2923	-0.0562	0.0276	0.0455	-0.0346	0.0069	-0.0058

$\frac{Y_1}{a}$	$\frac{Y_2}{a}$	$\frac{Y_3}{a}$	$\frac{Q_1}{a}$	$\frac{Q_2}{a}$	$\frac{Q_3}{a}$
-10.52	1.93	-1.37	99.41	3.18	-1.76

Table 1 lists the force constant values, as derived from the fitting procedure. The value of δ_1 allows one to reproduce the experimental violation of the second-order Cauchy relations to within 3%. Accordingly, many-body effects are well described by the harmonic model potential. The phonon dispersion relations along the high symmetry directions of the Brillouin zone are shown in figure 1, together with the experimental data. The long-range interactions are essential in accounting for the large Friedel oscillations of the potential. No substantial improvement occurs in the fit by extending the range beyond the sixth-neighbour shell.

3. Thermoelastic and caloric properties

The thermoelastic properties of metals depend sensitively on the effective range of the anharmonic potential. The vibrating atoms sample, in their temperature dependent

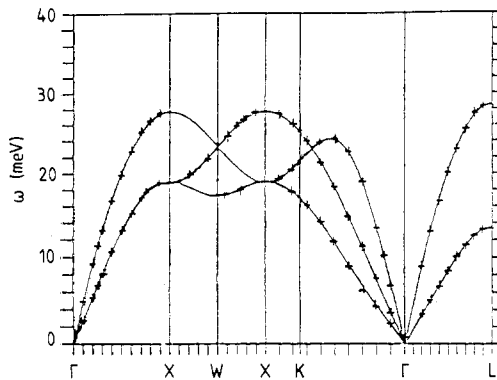


Figure 1. Phonon dispersion relations in Pd, along the symmetry directions of the Brillouin zone. + denotes the room-temperature experimental values (Miiller and Brockhouse 1971).

displacements, regions whose extension is related to the crystal equilibrium volume. Therefore, the volume dependence of the Helmholtz free energy should be fully taken into account in order to reproduce experiments.

The effects of strain on the atomic mean positions can be introduced in the crystal Hamiltonian by writing the phonon displacement fields as a superposition of microscopic vibrations inside the unit cell and macroscopic deformations of the cell itself (Barron and Klein 1974). This approach allows one to obtain a perturbative term $F_1(V, T)$ in the Helmholtz free energy as a function of the strain Hamiltonian H_s

$$F_1 = \beta^{-1} \left\langle T_\tau \left(\int_0^\beta d\tau_1 H_s(\tau_1) - \frac{1}{2} \int_0^\beta d\tau_1 \int_0^\beta d\tau_2 H_s(\tau_1) H_s(\tau_2) \right) S(\beta) \right\rangle_{0, \text{conn}} \quad (3)$$

with

$$S(\beta) = 1 - \int_0^\beta d\tau' H_{\text{anh}}(\tau') \quad (4)$$

where β is the inverse temperature, $\langle \dots \rangle_{0, \text{conn}}$ denotes that quantum averages are made on the unperturbed (harmonic) eigenstates of the crystal Hamiltonian and only connected diagrams may be retained. Thermal averages are implied by the formalism.

The full set of equations which relate H_s to the anharmonic force constant tensors is given by Zoli and Bortolani (1990). Here, I only point out that to lowest order H_s is quadratic in the normal coordinates expansion. Therefore, the constant-volume anharmonic Hamiltonian (H_{anh}), which consists of cubic and quartic terms in the normal coordinates, can be reasonably neglected in (4) and the use of the QHA is justified. In this view, the thermoelastic properties represent the anharmonic crystal response to perturbations induced by homogeneous deformations. Explicit expressions of linear thermal expansion coefficient $\alpha(T)$, isothermal bulk modulus $B^T(T)$ and mode Grüneisen parameters $\gamma(\mathbf{q}j)$, as functions of the cubic anharmonic force constants are given elsewhere (Zoli 1990). Zoli and Bortolani (1990), have also shown that the quartic anharmonic force constants scarcely affect thermoelastic properties of metallic systems.

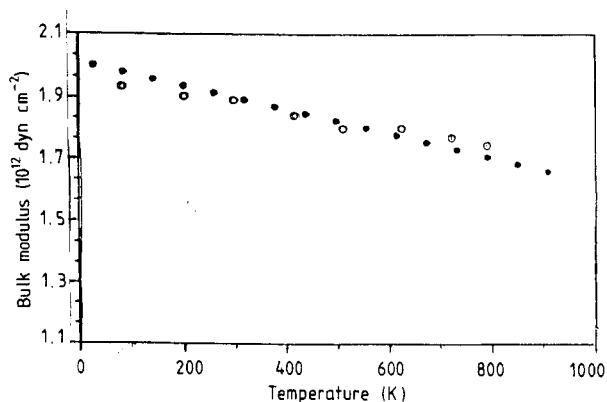


Figure 2. Linear thermal expansion coefficient versus temperature in Pd. ●, theoretical values; ○, experimental values (Touloukian *et al* 1970).

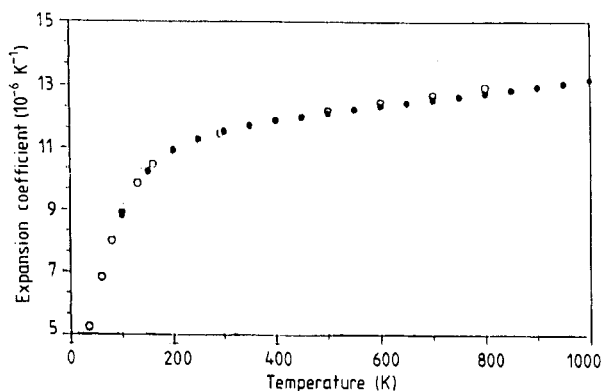


Figure 3. Isothermal bulk modulus versus temperature in Pd. ●, theoretical values; ○, experimental values (Landolt-Börnstein 1984).

I have determined the third-order derivatives of the pair potential in Pd, by fitting the experimental $\alpha(T)$ at three selected temperatures ($T = 100, 300, 800$ K). Although the high-temperature data could be well reproduced by a first-neighbour ranged cubic potential, the extension of the anharmonic interactions to third-neighbour atoms improves considerably the fitting in the low-temperature region. The values obtained for the three cubic force constants ($Y_i = r_i \phi'''(r_i)$ $i = 1, 2, 3$) are reported in table 1. These values have been used to calculate the temperature dependent $B^T(T)$ and the thermodynamic Grüneisen parameter γ_{td} . The resulting curves for $\alpha(T)$ and $B^T(T)$ are presented in figures 2 and 3, respectively, together with experimental data. In table 2, some computed values of γ_{td} and of the temperature derivative of the bulk modulus are reported. The fair agreement between theory and experiment proves that the QHA deals satisfactorily with thermal dilation effects in Pd. The higher-order terms (related to H_{anh}) yield contributions to the thermoelastic properties which are smaller by three orders of magnitude up to the melting temperature (T_m).

It should be noted that in alkali-halide (AH) and rare-gas (RG) solids, the higher-order corrections are relevant even at temperatures $T \simeq \frac{1}{3}T_m$ (Glyde and Klein 1971). Such a different behaviour can be attributed to the fact that the interatomic potentials in AH and RG solids have much steeper repulsive cores than potentials in metals. As a

Table 2. Calculated thermodynamic Grüneisen parameter γ_{td} , experimental value of γ_{td} (Gschneider 1964), calculated temperature derivative of the isothermal bulk modulus $dB^T(T)/dT$ in units of $10^7 \text{ N m}^{-2} \text{ K}^{-1}$. Zero-pressure experimental values of $dB^T(T)/dT$ (Weinmann and Steinemann 1974). Computed values of the constant-volume anharmonic specific heat in units of $\text{J K}^{-1} \text{ mol}^{-1}$.

T (K)	γ_{td}	γ_{td}	$\frac{dB^T(T)}{dT}$	$\left(\frac{dB^T(T)}{dT}\right)_{P=0}$	C_V^{anh}
100	2.20		-2.84		0.09
295	2.23	2.28 ± 0.1	-2.87	-2.51	0.69
800	2.24		-2.88	-2.55	1.33
1400	2.24		-2.88		1.36

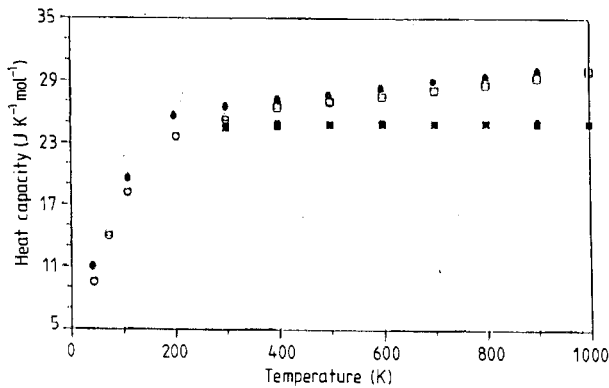


Figure 4. Constant pressure specific heat versus temperature in Pd. ●, theoretical values for C_P ; ■, theoretical values for (C_V^h) . Experimental data for C_P : ○, Clusius and Schachinger (1947); □, Touloukian *et al* (1970).

consequence, the n th-order ($n \geq 3$) derivatives of the potential are much larger in AH and RG solids than in metals and, in the former systems, the QHA fails to determine the effective temperature dependence of the phonon frequencies.

With regard to caloric properties, the directly measured quantity is the constant-pressure specific heat $C_P(T)$, whose explicit expression is

$$C_P(T) = C_V^h(T) + C_V^{\text{anh}}(T) + 9TV\alpha^2(T)B^T(T) \quad (5)$$

where V is the crystal volume in the undeformed state, C_V^h and C_V^{anh} are the constant-volume harmonic and anharmonic specific heat, respectively. According to (5), accurate predictions for C_P can not be carried out within the QHA, since C_V^{anh} is directly related to the cubic and quartic terms in H_{anh} . Moreover, the quartic anharmonic term contributes to the first perturbative order in the S -matrix expansion and therefore its effect has to be taken into account. I have used the measured $C_P(T)$ at $T = 800 \text{ K}$ to derive the value of the fourth-order derivative of the pair potential in Pd. By extending the range of the quartic anharmonic potential beyond the first-neighbour shell, the leading fourth-order force constant does not undergo substantial modifications. The values of the quartic force constants ($Q_i = r_i^2 \phi''''(r_i)$ $i = 1, 2, 3$) are listed in table 1. Theoretical and experimental $C_P(T)$ versus temperature are reported in figure 4. The harmonic contribution is also separately shown to emphasize effects of anharmonicities above room temperature. Some computed values of C_V^{anh}

are presented in table 2. Unlike noble metals (Martin 1987, Rosèn and Grimvall 1983) and aluminum (Leadbetter 1968), C_V^{anh} is positive in Pd. This result would suggest that a decreasing Debye temperature as a function of T , has also to be expected for this metal below room temperature.

4. Phonon lineshifts and linewidths

Due to anharmonicity the frequencies $\omega(\mathbf{q}j)$ of phonons, with wavevector \mathbf{q} and mode index j , are volume and temperature dependent. To lowest order in perturbation theory the harmonic frequencies ω_0 shift to

$$\omega(\mathbf{q}j) = \omega_0(\mathbf{q}j) + \Delta_T(\mathbf{q}j)$$

with

$$\Delta_T(\mathbf{q}j) = \Delta^{(0)}(\mathbf{q}j) + \Delta^{(3)}(\mathbf{q}j) + \Delta^{(4)}(\mathbf{q}j). \tag{6}$$

The dilation effects are provided by $\Delta^{(0)}(\mathbf{q}j)$ which can be written as

$$\Delta^{(0)}(\mathbf{q}j) = -3\alpha(T)T\gamma(\mathbf{q}j)\omega_0(\mathbf{q}j). \tag{7}$$

The terms $\Delta^{(4)}(\mathbf{q}j)$ and $\Delta^{(3)}(\mathbf{q}j)$ are the lowest-order contribution in the real part of the phonon self-energy. Their analytic expressions are

$$\begin{aligned} \Delta^{(4)}(\mathbf{q}j) &= \frac{12}{\hbar} \sum_{\mathbf{q}_1 j_1} V^{(4)}(\mathbf{q}j; \mathbf{q}_1 j_1; -\mathbf{q}_1 j_1; -\mathbf{q}j)(2n_1 + 1) \\ \Delta^{(3)}(\mathbf{q}j) &= -\frac{18}{\hbar^2} \sum_{\mathbf{q}_1, \mathbf{q}_2} \sum_{j_1, j_2} |V^{(3)}(-\mathbf{q}, j; \mathbf{q}_1, j_1; \mathbf{q}_2, j_2)|^2 \\ &\quad \times \text{PP} \left(\frac{n_1 + n_2 + 1}{\omega_0(\mathbf{q}j) + \omega_0(1) + \omega_0(2)} - \frac{n_1 + n_2 + 1}{\omega_0(\mathbf{q}j) - \omega_0(1) - \omega_0(2)} \right. \\ &\quad \left. + \frac{n_1 - n_2}{\omega_0(\mathbf{q}j) - \omega_0(1) + \omega_0(2)} - \frac{n_1 - n_2}{\omega_0(\mathbf{q}j) + \omega_0(1) - \omega_0(2)} \right) \end{aligned} \tag{8}$$

where PP denotes the principal value, $\omega_0(i) \equiv \omega_0(\mathbf{q}_i j_i)$, $n_i \equiv n(\omega_0(i))$ are the Bose-Einstein statistical factors and $V^{(3)}$ and $V^{(4)}$ are the Fourier transforms of the third- and fourth-order force constant tensors, respectively. The harmonic and anharmonic force constants of Pd, as determined in the previous sections, have been used here. As a consequence of translational invariance, the sums over two Brillouin zones in the second expression of (8) are reduced to a sum over \mathbf{q}_1 , with $\mathbf{q}_2 = \mathbf{q} - \mathbf{q}_1 + \mathbf{G}$ (\mathbf{G} is a reciprocal lattice vector). Numerical convergence in the third decimal place is achieved by using 8704 points in the entire Brillouin zone. The principal value has been represented by

$$\text{PP} \left(\frac{1}{x} \right) = \lim_{\epsilon \rightarrow 0} \frac{x}{x^2 + \epsilon^2} \tag{9}$$

with ϵ small but finite. $\Delta^{(3)}(\mathbf{q}j)$ results practically independent of ϵ over a range of values of ϵ . The value ($\epsilon = 0.18$ meV) that lies in the centre of such a range

has therefore been chosen. The terms in (7) and (8) have been computed at room temperature, with the wavevector \mathbf{q} lying along the symmetry directions $\{\xi 0 0\}$ and $\{\xi \xi 0\}$. In tables 3 and 4, the results are presented for transverse and longitudinal phonons, respectively. The agreement with the room-temperature experimental data, which are available for transverse (T_1) phonons, is satisfactory. The theory reproduces the enhanced softening of the transverse mode in the small \mathbf{q} region, along the $\{\xi \xi 0\}$ direction. Concerning the longitudinal phonons, the lineshifts are predicted to be peaked around the zone boundaries. Unlike the noble metals, the dilation term scarcely contribute to soften the phonon spectrum of Pd, whereas the cubic term $\Delta^{(3)}(\mathbf{q}j)$ provides the relevant effects.

Table 3. Lineshifts of transverse phonons in Pd. The shifts are in units of meV. The wavevectors are in units of $2\pi/a$. $\Delta^{(0)}$ is evaluated from (8); $\Delta^{(4)}$ and $\Delta^{(3)}$ are evaluated from (9); Δ_T , defined in (7), is calculated at room temperature. The experimental data are taken from Müller (1975). Along the $\{\xi \xi 0\}$ direction the data refer to the T_1 branch.

Wavevector \mathbf{q}	$\Delta^{(0)}$	$\Delta^{(4)}$	$\Delta^{(3)}$	Δ_T	Δ_T^{exp}
0.2 0.0 0.0	-0.119	-0.018	-0.548	-0.685	
0.4 0.0 0.0	-0.219	-0.033	-0.382	-0.634	
0.6 0.0 0.0	-0.291	-0.044	-0.551	-0.886	
0.8 0.0 0.0	-0.337	-0.051	-0.989	-1.377	
1.0 0.0 0.0	-0.354	-0.053	-0.95	-1.357	
0.15 0.15 0.0	0.031	-0.017	-0.252	-0.238	-0.175
0.30 0.30 0.0	0.046	-0.031	-0.992	-0.978	-0.910
0.45 0.45 0.0	0.039	-0.041	-0.671	-0.673	-0.512
0.60 0.60 0.0	0.016	-0.048	-0.622	-0.654	
0.75 0.75 0.0	0.011	-0.052	-0.561	-0.602	

Table 4. Lineshifts of longitudinal phonons in Pd. Symbols as defined in table 3.

Wavevector \mathbf{q}	$\Delta^{(0)}$	$\Delta^{(4)}$	$\Delta^{(3)}$	Δ_T
0.2 0.0 0.0	-0.047	-0.019	-0.413	-0.478
0.4 0.0 0.0	-0.091	-0.037	-0.663	-0.791
0.6 0.0 0.0	-0.127	-0.052	-0.956	-1.135
0.8 0.0 0.0	-0.150	-0.061	-1.750	-1.961
1.0 0.0 0.0	-0.158	-0.064	-1.431	-1.653
0.15 0.15 0.0	-0.063	-0.015	-0.541	-0.619
0.30 0.30 0.0	-0.112	-0.028	-0.575	-0.715
0.45 0.45 0.0	-0.137	-0.040	-1.222	-1.399
0.60 0.60 0.0	-0.132	-0.047	-2.070	-2.249
0.75 0.75 0.0	-0.134	-0.062	-1.989	-2.185

The phonon linewidths $\Gamma(\mathbf{q}j)$ may be obtained by applying the Kramers-Kronig relation to the second expression of (8). However, a better numerical convergence is obtained by computing directly the explicit formula as given in second-order perturbation theory

$$\Gamma(\mathbf{q}j) = \frac{18\pi}{\hbar^2} \sum_{\mathbf{q}_1, \mathbf{q}_2} \sum_{j_1, j_2} |V^{(3)}(-\mathbf{q}, j; \mathbf{q}_1, j_1; \mathbf{q}_2, j_2)|^2 \{(n_1 + n_2 + 1)\}$$

$$\begin{aligned} & \times [\delta(\omega_0(\mathbf{qj}) - \omega_0(1) - \omega_0(2)) - \delta(\omega_0(\mathbf{qj}) + \omega_0(1) + \omega_0(2))] \\ & + (n_1 - n_2)[\delta(\omega_0(\mathbf{qj}) + \omega_0(1) - \omega_0(2)) - \delta(\omega_0(\mathbf{qj}) - \omega_0(1) + \omega_0(2))] \end{aligned} \quad (10)$$

As noted above, the double sums are reduced to a sum over \mathbf{q}_1 because of translational invariance. The δ -functions have been represented as follows:

$$\delta[f_l(x)] = \sum_n \frac{\delta(x - x_n)}{|f'_l(x_n)|} \quad l = 1, 2, 3 \quad (11)$$

with

$$\begin{aligned} f_1(q_{1,z}) &= \omega_0(\mathbf{qj}) - \omega_0(q_{1,x}, q_{1,y}, q_{1,z}; j_1) - \omega_0(q_x - q_{1,x}; q_y - q_{1,y}; q_z - q_{1,z}; j_2) \\ f_2(q_{1,z}) &= \omega_0(\mathbf{qj}) + \omega_0(q_{1,x}, q_{1,y}, q_{1,z}; j_1) - \omega_0(q_x - q_{1,x}; q_y - q_{1,y}; q_z - q_{1,z}; j_2) \\ f_3(q_{1,z}) &= \omega_0(\mathbf{qj}) - \omega_0(q_{1,x}, q_{1,y}, q_{1,z}; j_1) + \omega_0(q_x - q_{1,x}; q_y - q_{1,y}; q_z - q_{1,z}; j_2). \end{aligned} \quad (12)$$

For a fixed point $(q_{1,x}, q_{1,y})$ the argument of the δ -function depends on the one-dimensional variable $q_{1,z} = x$. In (11), the sum over the zeroes x_n , which ensure energy conservation in the three phonon scattering processes, ranges from 1 to 4 for a given point $(q_{1,x}, q_{1,y})$. Therefore, by using 3104 points in the plane (x, y) , I can sample around 10 000 points in the entire Brillouin zone. Umklapp processes have to be taken into account since their number is comparable to the number of normal processes. The derivatives of $f_l(x)$ never vanish at the zeroes x_n so that focussing effects are not present in the bulk of Pd. In table 5, the computed linewidths of longitudinal and transverse phonons are reported together with the available room-temperature experimental data along the $[\xi\xi 0]T_1$ branch. The calculated linewidths of transverse phonons are in fair agreement with the measured values. Similarly to Al and Au, an enhanced decay process for the $(0.8 \ 0.0 \ 0.0)$ longitudinal mode is also found in Pd. However, only low-temperature (4.6 K) measurements are available for longitudinal phonons along the $[\xi 00]$ direction. According to this data, the maximum width is observed at $\xi = 0.4$.

Table 5. Room temperature linewidths for Pd in units of meV. Along the $[\xi\xi 0]$ direction the data refer to the T_1 branch. The experimental data are taken from Miiller (1975).

Wavevector \mathbf{q}	2Γ		$2\Gamma^{\text{exp}}$
	Longitudinal	Transverse	
0.2 0.0 0.0	0.154	0.094	
0.4 0.0 0.0	0.519	0.236	
0.6 0.0 0.0	1.155	0.694	
0.8 0.0 0.0	1.871	0.853	
1.0 0.0 0.0	1.740	0.801	
0.15 0.15 0.0	0.382	0.187	
0.30 0.30 0.0	0.666	0.653	0.745
0.45 0.45 0.0	1.297	0.803	0.830
0.60 0.60 0.0	1.327	0.558	0.620
0.75 0.75 0.0	1.073	0.532	

At room temperature the phonon-phonon scattering should provide the predominant contribution to the decay rate while at low temperatures the electron-phonon scattering should play a relevant role (Youngblood *et al* 1979). Moreover, the former mechanism should determine the linewidths for large momenta q while the latter should be dominant for small momenta. Since the linewidths of longitudinal phonons are strongly q dependent along the $[\xi 00]$ direction, it would be worthwhile to obtain experimental information concerning this q dependence as a function of temperature. This research may greatly help to quantify the effects of the different sources of scattering on the anharmonic properties of FCC metals.

Acknowledgments

I am grateful to T Chivone for many useful discussions and to F Richter for his valuable collaboration.

References

- Barron T H K and Klein M L 1974 *Dynamical Properties of Solids* ed G K Horton and A A Maradudin (Amsterdam: North Holland)
- Clusius K and Schachinger L 1947 *Z. Naturf.* a **2** 90
- Daw M S and Baskes M I 1983 *Phys. Rev. Lett.* **50** 1285
- Daw M S and Hatcher R D 1985 *Solid State Commun.* **56** 697
- Ercolessi F, Tosatti E and Parrinello M 1986 *Phys. Rev. Lett.* **57** 719
- Foiles S M and Adams J B 1989 *Phys. Rev. B* **40** 5909
- Foiles S M, Baskes M I and Daw M S, 1986 *Phys. Rev. B* **33** 7983
- Gschneider K A 1964 *Solid State Physics* ed F Seitz and D Turnbull (New York: Academic)
- Kohn W 1959 *Phys. Rev. Lett.* **2** 393
- Landolt-Börnstein New Series* 1984 vol 18 (Berlin: Springer)
- Leadbetter A J 1968 *J. Phys. C: Solid State Phys.* **1** 1489
- Martin D L 1987 *Can. J. Phys.* **65** 1104
- Miiller A P 1975 *Can. J. Phys.* **53** 2491
- Miiller A P and Brockhouse P N 1968 *Phys. Rev. Lett.* **20** 798
- Miiller A P and Brockhouse P N 1971 *Can. J. Phys.* **49** 704
- Pinski F J and Butler W H 1979 *Phys. Rev. B* **19** 6010
- Rosèn J and Grimvall G 1983 *Phys. Rev. B* **27** 7199
- Ting N, Quingliang Y and Yiyang Y E 1988 *Surf. Sci.* **206** L857
- Touloukian Y S, Kirby R K, Taylor R E and Lee T Y R 1970 *Thermophysical Properties of Matter* vols 4, 12 (New York: Plenum)
- Weinmann C and Steinemann S 1974 *Solid State Commun.* **15** 281
- Youngblood R, Noda Y and Shirane G 1979 *Phys. Rev. B* **19** 6016
- Zoli M 1990 *Phys. Rev. B* **41** 7497
- Zoli M and Bortolani V 1990 *J. Phys.: Condens. Matter* **2** 525
- Zoli M, Santoro G, Bortolani V, Maradudin A A and Wallis R F 1990 *Phys. Rev. B* **41** 7507